

Detrital zircons reveal sea-level and hydroclimate controls on Amazon River to deep-sea fan sediment transfer

Cody C. Mason¹, Brian W. Romans², Daniel F. Stockli³, Russel W. Mapes⁴, and Andrea Fildani⁵

¹Department of Geosciences, University of West Georgia, Callaway Building, 1601 Maple St., Carrollton, Georgia 30118, USA

²Department of Geosciences, Virginia Tech, 4044 Derring Hall, 926 W. Campus Dr., Blacksburg, Virginia 24061, USA

³Department of Geological Sciences, The University of Texas at Austin, 1 University Station C1100, Austin, Texas 78712, USA

⁴ExxonMobil, 22777 Springwoods Village Pkwy, Spring, Texas 77389, USA

⁵Equinor Research Center, Austin, Texas 78730, USA

ABSTRACT

We use new U-Pb detrital zircon (DZ) geochronology from the Pleistocene Amazon submarine fan ($n = 1352$ grains), integrated with onshore DZ age data, to propose a sedimentary model for sea level–modulated and hydroclimate–modulated sediment transfer in Earth’s largest source-to-sink system. DZ ages from the modern Amazon River sediment display a progressive downstream dilution by older cratonic zircons, leading to the expectation of a submarine fan with high proportions of craton-derived sediment. Our new DZ age data from the submarine fan and mixture modeling suggest that higher proportions of sediment were supplied from the distant central Andes to the Amazon fan during the last two glacioeustatic lowstands, and thus the observed DZ age spectra of the modern lower Amazon River indicate a relative increase in craton-derived sediment during the Holocene. We interpret that during interglacials, when sea level was high and the submarine fan inactive, the lower Amazon River did not efficiently transfer sand-sized sediment to the margin and thus became enriched in craton-derived sediment. During sea-level lowstands, increased gradients and incision in the lower Amazon River due to base-level lowering resulted in enhanced connectivity and transfer of Andes-sourced zircons to the deep sea. These results are also consistent with interpreted patterns of Andean–Amazon hydroclimate anti-phasing (enhanced precipitation in the central Andes and increased aridity in the northern Amazon Basin) during the Last Glacial Maximum. Our results suggest that sand-sized sediment in the Amazon submarine fan records multi-millennial patterns of sea level and South American hydroclimate.

INTRODUCTION

The dynamics of fluvial to deep-sea sediment transfer in response to climate and sea-level fluctuations over multi-millennial time scales is complex and nonlinear (Blum and Törnqvist, 2000; Clift, 2006; Blum and Hattier-Womack, 2009). Early research on major fluvial systems focused on the role of base level (Vail et al., 1977) in the context of climate change (Fisk, 1944), while subsequent research modified conceptual models in recognition of the influence of upstream climate-modulated sediment supply and hydrology (Saucier, 1996). Other studies have considered the controls on the timing of submarine fan activity (Covault and Graham, 2010; Maslin, 2009), sediment caliber and volumes delivered to submarine fans (Sweet and Blum, 2016), as well as sediment exhumation and transit rates and the role of river

avulsions in sediment transfer to the deep sea (Blum et al., 2018). Provenance techniques applied to major river-to-submarine fan systems are a valuable tool to improve models for the controls on source-to-sink sediment routing system behavior over multi-millennial time scales (Fildani et al., 2018).

The Amazon River and deep-sea fan represent a globally important end-member system for understanding land-to-sea sediment dynamics. Submarine fans have been shown to archive histories of output fluxes and onshore environmental change (Normark and Reid, 2003; Fildani et al., 2016; Hessler et al., 2018), and have been used to invert up-system climate forcings in glaciated continent-scale rivers (Clift et al., 2008; Fildani et al., 2016, 2018; Mason et al., 2017; Li et al., 2019). The Amazon catchment straddles equatorial latitudes and has dis-

tinct sediment and detrital zircon (DZ) source terranes and physiography (Fig. 1), and the modern fluvial system is characterized by published DZ U-Pb data (Fig. 1B) (Campbell and Allen, 2008; Mapes, 2009; Pepper et al., 2016).

We present 1352 new U-Pb DZ ages from 10 samples from cores recovered in the deep-sea Amazon Fan (Sites 936, 945, 946) during Ocean Drilling Program (ODP) Leg 155 (Flood et al., 1995). We integrate our data and results with published U-Pb DZ data from the modern onshore Amazon fluvial system and perform mixture modeling of DZ age spectra to elucidate effects of changing sea level and hydroclimate on temporal patterns of sediment provenance over multi-millennial time scales (marine isotope stages 6–2; MIS 6–MIS 2) within Earth’s largest fluvial to deep-sea sediment routing system.

THE AMAZON SOURCE-TO-SINK SYSTEM

The Amazon River represents Earth’s largest freshwater discharge to the ocean (15%–20% of global total) and largest total sediment load (~1200 Mt/yr), and is the largest fluvial system in terms of drainage basin area (~ 7×10^6 km²) (Milliman and Farnsworth, 2011). Amazon Basin hydroclimate controls water and sediment discharge to the sea and is influenced by the South American monsoon system and the locations of the Intertropical Convergence Zone and South Atlantic Convergence Zone (Novello et al., 2017). Hydroclimate in the central and northern Amazon Basin was overall more arid during the Last Glacial Maximum (LGM) (Häggi et al., 2017), while precipitation increased for the central Andes and the southeastern Amazon craton (Cheng et al., 2013; Baker and Fritz, 2015). Amazon floodplain incision during the LGM significantly altered the ele-

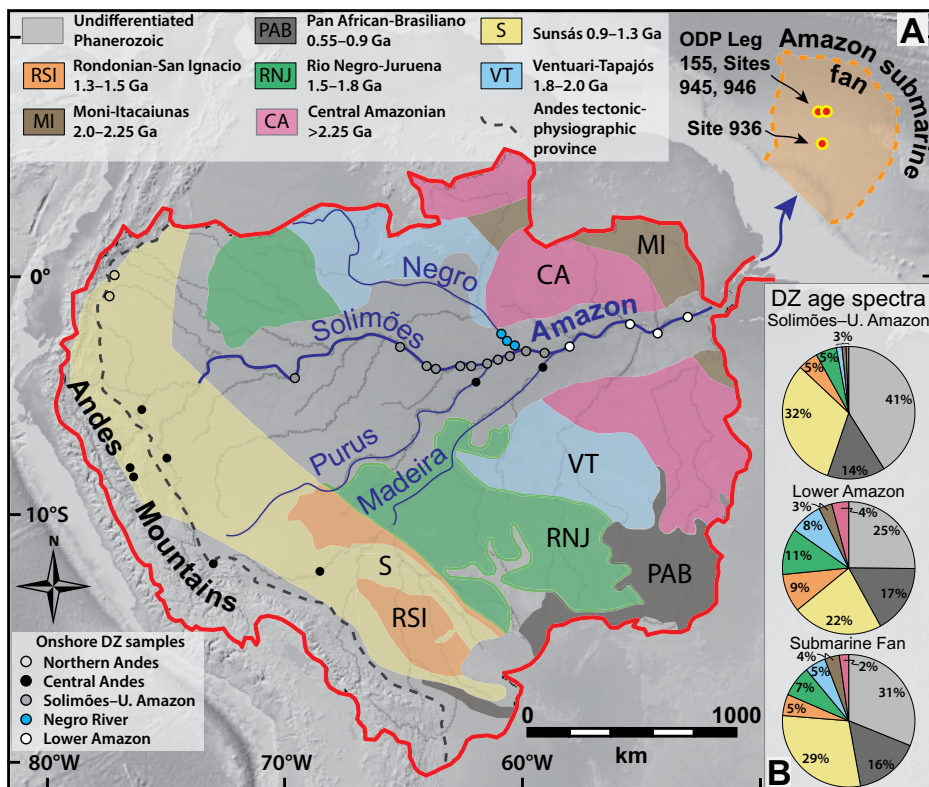


Figure 1. A: Physiography and simplified detrital zircon (DZ) source terrane map of Amazon catchment and submarine fan system, with major fluvial elements of Amazon River system, existing onshore DZ sample locations (Campbell and Allen, 2008; Mapes, 2009; Pepper et al., 2016), and locations of Ocean Drilling Program (ODP) sediment cores used in this study. Geology adapted is from Chew et al. (2011, and references therein), and fan extents are from Damuth et al. (1995). B: Pie diagrams with percentages for U-Pb DZ ages from samples in Solimões–upper Amazon River, lower Amazon River, and Amazon Fan.

vation and slope of the river bed in the lower Amazon River (i.e., from ~0.7 to ~7 cm/km) (Mertes and Dunne, 2007). The degree of upstream propagation of incision is uncertain, but may have influenced bed elevations as far as 1700 km from the modern coast (Mertes and Dunne, 2007).

The Amazon submarine fan is a late Miocene through Pleistocene accumulation of mainly terrigenous siliciclastic sediment as much as 4–5 km thick (Figueiredo et al., 2009). During highstands, coarse-grained sediment is deposited and stored in floodplains in the lower Amazon River valley and on the shallow continental shelf. When sea levels fall by >40 m relative to Holocene sea level, river water and sediment is transferred across the continental shelf and through the Amazon canyon to the submarine fan (Damuth et al., 1995).

The modern onshore Amazon system is partially constrained by existing detrital geochronology (Figs. 1A and 1B) (Campbell and Allen, 2008; Mapes, 2009; Pepper et al., 2016). DZ age data from the Solimões (upper Amazon) and lower Amazon Rivers (Fig. 1A) display a progressive dilution of young zircon age modes (<1.3 Ga) by older craton age modes (Fig. 1B). Given the observed pattern of downstream di-

lution by cratonic zircon sources, we might expect a submarine fan enriched in a cratonic DZ signature.

METHODS AND RESULTS

We collected 10 samples of fine- to medium-grained sand from turbidite beds in cores recovered during ODP Leg 155 (Flood et al., 1995), Sites 936, 945, and 946, in the lower Amazon Fan (Fig. 1A for locations; Data File DR1 in the GSA Data Repository¹). All sample preparation, analyses, and data reduction were conducted at the UTChron facility at the University of Texas at Austin (USA), where we used standard techniques of mineral separation, and applied laser ablation–inductively coupled plasma–mass spectrometry U-Pb dating of zircon grains (methods of Thomson et al. [2017] and references therein).

¹GSA Data Repository item 2019206, DR1 (Ocean Drilling Program Amazon fan samples); DR2 (Amazon detrital zircon data); DR3 (published detrital zircon samples used in mixture models); and DR4 (unmixing coefficients for detrital zircon samples from the modern lower Amazon and Pleistocene Amazon submarine fan), is available online at <http://www.geosociety.org/datarepository/2019/>, or on request from editing@geosociety.org.

Resultant DZ ages are presented within their composite stratigraphic context (Fig. 2A) as kernel density estimates (KDEs; Figs. 2B and 2C) and plotted using a multidimensional scaling (MDS) map (Fig. 2D). Full isotopic measurements are reported in Data File DR2.

The MDS map (Fig. 2D) indicates that the Amazon Fan is a mixture of Andean and cratonic sources, and is most closely related to the central Andes, lower Amazon, and craton sources in MDS space. Sample KDEs from the Amazon Fan (Fig. 2B) show little evidence for systematic stratigraphic trends, but display variable proportions of Phanerozoic and Pan-African–Brasiliano age modes (Fig. 2B). KDE cross-correlation coefficients for all Amazon Fan samples (see Table DR2 in the Data Repository) have a mean and standard deviation (1σ) of 0.45 ± 0.08 , which is similar to or slightly less than coefficients for synthetic subsamples drawn from the same parent sample (Saylor and Sundell, 2016).

Collectively, Amazon Fan DZ samples (Fig. 2C) have age modes nearly identical to those of published samples from the Amazon River (Mapes, 2009; Campbell and Allen, 2008) (Fig. 2C). However, (1) fan samples are qualitatively more homogenous than modern samples from the length of Amazon River, and (2) Amazon Fan DZ age spectra contain higher proportions of Phanerozoic through Sunsás orogeny–aged zircons (76% U-Pb ages <1.3 Ga) than samples from the lower Amazon (64% <1.3 Ga) (Figs. 1B and 2D; Table DR1), while the modern lower Amazon contains higher proportions of >1.3 Ga zircons derived from the craton (Fig. 1B).

To further explore this observed variability in provenance signature between Holocene river and Pleistocene submarine fan samples, we applied a top-down unmixing algorithm (*sensu* Sharman and Johnstone, 2017; after Mason et al., 2017; Fildani et al., 2018) to quantify the relative contributions of zircons from tributary river components (parents) present in composite (daughter) mixtures, or the lower Amazon River and Amazon Fan. We selected published DZ samples (Campbell and Allen, 2008; Mapes, 2009; Pepper et al., 2016) based on their geographic locations within the Amazon drainage basin, with the goal of characterizing broad swaths of DZ terranes using modern river sands. Results can be viewed in terms of supply from the northern Andes, the northern craton (samples from the Negro River), and the central Andes (Fig. 1A; also see the Data Repository text and Table DR3).

Unmixing amalgamated samples from the modern lower Amazon River results in large proportions of the craton component (67%) and moderate proportions of the central Andes component (33%) (Table DR4). Unmixing amalgamated samples from the Pleistocene Amazon Fan (spanning MIS 6–MIS 2) results in much smaller proportions of the craton component (17%) and

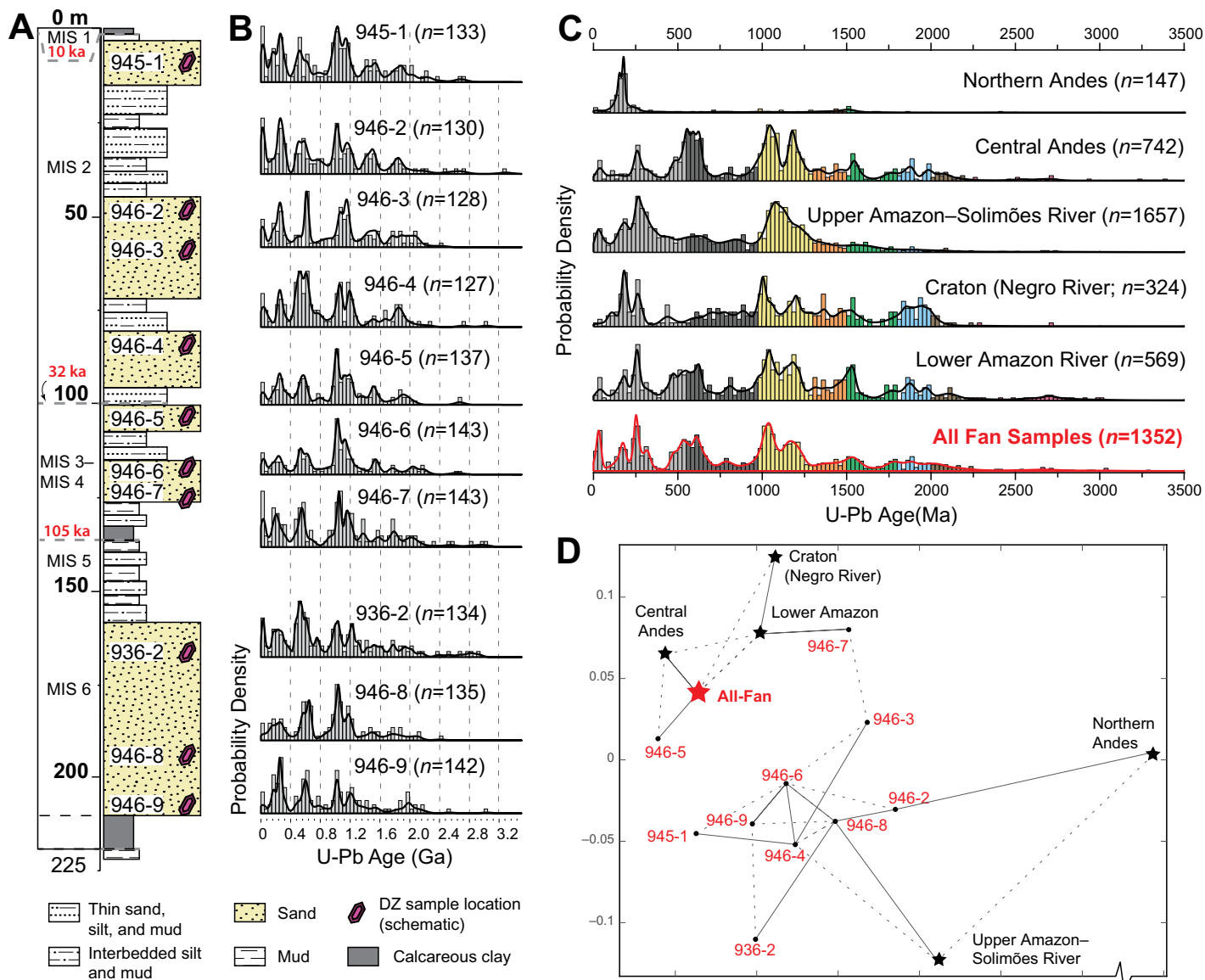


Figure 2. Results of U-Pb detrital zircon (DZ) geochronology from Amazon submarine fan. A: Composite stratigraphic section from Ocean Drilling Program (ODP) Leg 155, Sites 936, 945, and 946 (after Damuth et al., 1995; Flood et al., 1995), with interpreted ages of strata (red text), marine isotope stages (MIS), and schematic DZ sample locations. B: Kernel density estimates and histograms binned at 50 m.y. intervals from samples in A. C: Amalgamated U-Pb DZ geochronology from Amazon submarine fan, binned at 25 m.y. intervals, and compared to amalgamated DZ samples from Amazon River (Campbell and Allen, 2008; Mapes, 2009; Pepper et al., 2016). D: Metric multidimensional scaling (MDS) map for samples from Amazon submarine fan and fluvial network. Axes are expressions of dissimilarity based on Kolmogorov-Smirnov (K-S) effect size; similar samples cluster together, while dissimilar samples plot farther apart (methods of Vermeesch, 2013). Solid lines mark closest neighbors; dashed lines, second-closest neighbors.

greater proportions of the central Andes component (78%), with minor proportions of the northern Andes component (5%) (Table DR4).

DISCUSSION

U-Pb DZ ages from the Amazon Fan demonstrate that large tropical river-to-fan systems faithfully record their onshore catchment geology (Figs. 1A and 2C). Contrary to the expectation that Amazon Fan sediment should reflect the proportions of zircons present in the lower Amazon River, our DZ age data and mixing models suggest that the Pleistocene submarine fan contains higher proportions of northern and

central Andes-derived sediment than modern samples from the lower Amazon River (Fig. 1B).

We hypothesize that more efficient transfer of northern and central Andean sediment to the submarine fan during glacial lowstand is facilitated by changes in Amazon River morphology driven by falling base level and by Pleistocene hydroclimate variability (Fig. 3). The sediment trapping capacity of the lower Amazon River at high sea level must have been significantly reduced during the LGM and previous global glacioeustatic lowstands, when incision led to increased channel gradients along >1000 km of the lower Amazon River (Mertes and Dunne,

2007), decreased sediment retention in tributary and main-stem floodplains, and recycling and evacuation of the river valley and coastal zone deposits (Fig. 3A). Moreover, enhanced precipitation in the Andes relative to the craton during the LGM (MIS 2) (Baker and Fritz, 2015) may have led to higher erosion rates and increased transport of Andean detritus across the continent and ultimately to the submarine fan. Age data and mixture model results from MIS 6 deposits suggest a similar configuration during the penultimate glacioeustatic lowstand. We hypothesize that the signal of cratonic enrichment in the lower Amazon during highstands would

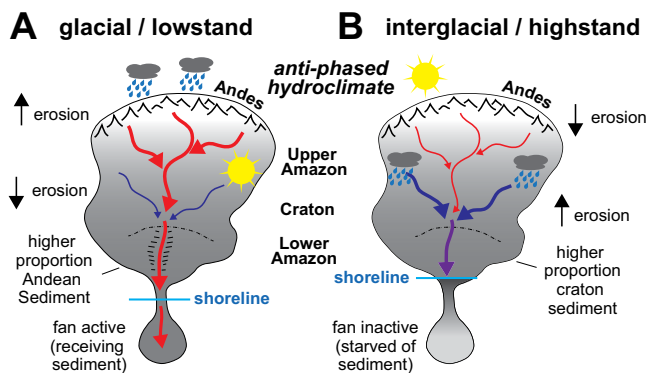


Figure 3. Interpreted relationships between sea level, Andes-Amazon hydroclimate, and resultant changes in sediment production and transfer through fluvial network to deep-sea across glacial (A) and interglacial (B) phases. Arrows indicate direction of change in erosion rate in the Andes and the Amazon craton (up = increase in erosion, down = decrease).

have been effectively diluted by significantly higher proportions of Andean sources during lowstands as well as potential thorough mixing of grain populations during transport in marine turbidity currents, and, thus, would not be detectable in the fan record.

Studies of the fine-grained fraction of terrigenous marine sediment support our proposed model. Nd and Pb isotopic measurements of mud from the Amazon Fan (McDaniel et al., 1997) and Pb isotopes from the adjacent Ceará Rise (Abouchami and Zabel, 2003) suggest that fine terrigenous material is derived mainly from Andean highlands. Marine deposits on the Ceará Rise display Milankovitch cyclicity, with increased Andean inputs during glacioeustatic lowstands and increased cratonic inputs during glacioeustatic highstands (Abouchami and Zabel, 2003), suggesting a strong link between terrestrial climate, spatial patterns of erosion, and sediment routing system behavior.

Our DZ data are representative of the sand-sized fraction of sediment produced within the Amazon catchment and transferred to the deep-sea during glacial lowstands, and thus our interpretations rely on assumptions of the representative nature of U-Pb DZ geochronology from modern river sands and marine sediment. Grain-size variations may influence DZ age populations (Ibañez-Mejía et al., 2018), but amalgamating multiple published river samples should smooth potential grain-size effects, and turbidite deposits sampled from the fan were a consistent grain size (dominantly fine sand). Variable Zr content across source terranes or drainage basins (e.g., zircon fertility; Moecher and Samson, 2006) would affect calculated proportions of erosion versus sediment supply (Amidon et al., 2005; Spencer et al., 2018). However, the temporal variation in our calculated relative sediment loads from distinct source areas in the Amazon system cannot be related to fertility, as source terrane fertility does not change temporally. Rather, these variations must be the result of changes in the proportion of sediment from distinct source areas in the Amazon catchment.

New data from the Pleistocene Amazon Fan yield similar results to studies in the Indus River

source-to-sink system, where variable monsoonal intensity since the LGM has resulted in measurable changes in provenance of sediment from cores along the delta and in the submarine canyon (Clift et al., 2008; Clift and Giosan, 2014; Li et al., 2019). In North America, continental ice-sheet dynamics modulated the Pleistocene Mississippi River–Missouri River drainage system and resulted in major variation of provenance signatures and overall sediment delivery to the Mississippi submarine fan (Fildani et al., 2018; Hessler et al., 2018). Here we note the relatively surprising result that the Amazon Fan appears to archive a consistent record of glacial sea levels and terrestrial hydroclimate of South America, rather than the expected sediment mixture present in the lower Amazon today.

CONCLUSIONS

The Pleistocene Amazon Fan archives a record of sediment transfer and provenance related to glacial-interglacial eustatic sea levels and the dominant terrestrial hydroclimate of South America at multi-millennial time-scales. U-Pb detrital zircon geochronology (DZ; $N = 10$ samples, $n = 1352$ grains) from the Pleistocene submarine fan suggest that Andean sediment was more efficiently transferred across the South American continent to the deep sea during Pleistocene glacial intervals. This was potentially facilitated by South America hydroclimate anti-phasing: enhanced precipitation and erosion of the central Andes during glacial maxima, while increased aridity in much of the Amazon Basin led to decreased weathering and erosion rates. Enhanced Andean sediment loads in the Amazon River during glacial lowstands would have coincided with incision and increased channel gradients along the lower 1200 km of the Amazon River. The higher proportion of craton-derived DZs in the modern lower Amazon River may be explained by enhanced precipitation and sediment production on the craton, and potentially more net storage of Andes-derived detritus in upstream locations during highstands. Our results highlight the value of source-to-sink studies of river to submarine-fan systems that record changing and dominant terrestrial conditions.

ACKNOWLEDGEMENTS

Funding for analyses and CM's postdoctoral fellowship was provided by Equinor, and we thank Mason Dykstra for supporting the project. Lisa Stockli provided assistance in the laboratory. Glenn Sharman, Ken Eriksson, and Mark Maslin provided helpful discussions. We thank *Geology* Science Editor Mark Quigley. We thank Liviu Giosan, Chris Hawkesworth, Débora Nascimento, and two anonymous reviewers for insightful comments that helped shape and strengthen this manuscript.

REFERENCES CITED

- Abouchami, W., and Zabel, M., 2003, Climate forcing of the Pb isotope record of terrigenous input into the equatorial Atlantic: Earth and Planetary Science Letters, v. 213, p. 221–234, [https://doi.org/10.1016/S0012-821X\(03\)00304-2](https://doi.org/10.1016/S0012-821X(03)00304-2).
- Amidon, W.H., Burbank, D.W., and Gehrels, G.E., 2005, Construction of detrital mineral populations: Insights from mixing of U-Pb zircon ages in Himalayan rivers: Basin Research, v. 17, p. 463–485, <https://doi.org/10.1111/j.1365-2117.2005.00279.x>.
- Baker, P.A., and Fritz, S.C., 2015, Nature and causes of Quaternary climate variation of tropical South America: Quaternary Science Reviews, v. 124, p. 31–47, <https://doi.org/10.1016/j.quascirev.2015.06.011>.
- Blum, M.D., and Hattier-Womack, J., 2009, Climate change, sea-level change, and fluvial sediment supply to deepwater depositional systems, in Kneller, B., et al., eds., External Controls on Deep-Water Depositional Systems: SEPM (Society for Sedimentary Geology) Special Publication 92, p. 15–39, <https://doi.org/10.2110/sepmssp.092.015>.
- Blum, M.D., and Törnqvist, T.E., 2000, Fluvial responses to climate and sea-level change: A review and look forward: Sedimentology, v. 47, p. 2–48, <https://doi.org/10.1046/j.1365-3091.2000.00008.x>.
- Blum, M., Rogers, K., Gleason, J., Najman, Y., Cruz, J., and Fox, L., 2018, Allogenic and autogenic signals in the stratigraphic record of the deep-sea Bengal Fan: Scientific Reports, v. 8, 7973, <https://doi.org/10.1038/s41598-018-25819-5>.
- Campbell, I.H., and Allen, C.M., 2008, Formation of supercontinents linked to increases in atmospheric oxygen: Nature Geoscience, v. 1, p. 554–558, <https://doi.org/10.1038/ngeo259>.
- Cheng, H., Sinha, A., Cruz, F.W., Wang, X., Edwards, R.L., D'Horta, F.M., Ribas, C.C., Vuille, M., Stott, L.D., and Auler, A.S., 2013, Climate change patterns in Amazonia and biodiversity: Nature Communications, v. 4, 1411, <https://doi.org/10.1038/ncomms2415>.
- Chew, D.M., Cardona, A., and Mišković, A., 2011, Tectonic evolution of western Amazonia from the assembly of Rodinia to its break-up: International Geology Review, v. 53, p. 1280–1296, <https://doi.org/10.1080/00206814.2010.527630>.
- Clift, P.D., 2006, Controls on the erosion of Cenozoic Asia and the flux of clastic sediment to the ocean: Earth and Planetary Science Letters, v. 241, p. 571–580, <https://doi.org/10.1016/j.epsl.2005.11.028>.
- Clift, P.D., and Giosan, L., 2014, Sediment fluxes and buffering in the post-glacial Indus Basin: Basin Research, v. 26, p. 369–386, <https://doi.org/10.1111/bre.12038>.
- Clift, P.D., et al., 2008, Holocene erosion of the Lesser Himalaya triggered by intensified summer monsoon: Geology, v. 36, p. 79–82, <https://doi.org/10.1130/G24315A.1>.
- Covault, J.A., and Graham, S.A., 2010, Submarine fans at all sea-level stands: Tectono-morphologic

- and climatic controls on terrigenous sediment delivery to the deep sea: *Geology*, v. 38, p. 939–942, <https://doi.org/10.1130/G31081.1>.
- Damuth, J.E., Flood, R.D., Pirmez, C., and Manley, P.L., 1995, Architectural elements and depositional processes of Amazon Deep-sea Fan imaged by long-range sidescan sonar (GLORIA), bathymetric swath-mapping (Sea Beam), high-resolution seismic and piston-core data, *in* Pickering, K.T., et al., eds., *Atlas of Deep Water Environments: Architectural Style in Turbidites*: Oxford, U.K., Chapman and Hall, p. 105–121, https://doi.org/10.1007/978-94-011-1234-5_19.
- Figueiredo, J., Hoorn, C., van der Ven, P., and Soares, E., 2009, Late Miocene onset of the Amazon River and the Amazon deep-sea fan: Evidence from the Foz do Amazonas Basin: *Geology*, v. 37, p. 619–622, <https://doi.org/10.1130/G25567A.1>.
- Fildani, A., McKay, M.P., Stockli, D., Clark, J., Dykstra, M.L., Stockli, L., and Hessler, A.M., 2016, The ancestral Mississippi drainage archived in the late Wisconsin Mississippi deep-sea fan: *Geology*, v. 44, p. 479–482, <https://doi.org/10.1130/G37657.1>.
- Fildani, A., Hessler, A.M., Mason, C.C., McKay, M.P., and Stockli, D.F., 2018, Late Pleistocene glacial transitions in North America altered major river drainages, as revealed by deep-sea sediment: *Scientific Reports*, v. 8, 13839, <https://doi.org/10.1038/s41598-018-32268-7>.
- Fisk, H.N., 1944, Geological investigation of the alluvial valley of the lower Mississippi River: Vicksburg, Mississippi, U.S. Department of the Army, Mississippi River Commission, 78 p.
- Flood, R.D., Piper, D.J.W., Klaus, A., et al., 1995, *Proceedings of the Ocean Drilling Program, Initial Reports, Volume 155*: College Station, Texas, Ocean Drilling Program, <https://doi.org/10.2973/odp.proc.ir.155.1995>.
- Hägg, C., Chiessi, C.M., Merkel, U., Mulitza, S., Prange, M., Schulz, M., and Schefuß, E., 2017, Response of the Amazon rainforest to late Pleistocene climate variability: *Earth and Planetary Science Letters*, v. 479, p. 50–59, <https://doi.org/10.1016/j.epsl.2017.09.013>.
- Hessler, A.M., Covault, J.A., Stockli, D.F., and Fildani, A., 2018, Late Cenozoic cooling favored glacial over tectonic controls on sediment supply to the western Gulf of Mexico: *Geology*, v. 46, p. 995–998, <https://doi.org/10.1130/G45528.1>.
- Ibañez-Mejía, M., Pullen, A., Pepper, M., Urbani, F., Ghoshal, G., and Ibañez-Mejía, J.C., 2018, Use and abuse of detrital zircon U-Pb geochronology—A case from the Río Orinoco delta, eastern Venezuela: *Geology*, v. 46, p. 1–4, <https://doi.org/10.1130/G45596.1>.
- Li, Y., Clift, P.D., and O’Sullivan, P., 2019, Millennial and centennial variations in zircon U-Pb ages in the Quaternary Indus Submarine Canyon: *Basin Research*, v. 31, p. 155–170, <https://doi.org/10.1111/bre.12313>.
- Mapes, R.W., 2009, Past and present provenance of the Amazon River drainage basin [Ph.D. thesis]: Chapel Hill, University of North Carolina, 185 p.
- Maslin, M., 2009, Review of the timing and causes of the Amazon-Fan mass transport and avulsion deposits during the latest Pleistocene, *in* Kneller, B., et al., eds., *External Controls on Deep-Water Depositional Systems: SEPM (Society for Sedimentary Geology) Special Publication 92*, p. 133–144, <https://doi.org/10.2110/sepm.092.133>.
- Mason, C.C., Fildani, A., Gerber, T., Blum, M.D., Clark, J.D., and Dykstra, M., 2017, Climatic and anthropogenic influences on sediment mixing in the Mississippi source-to-sink system using detrital zircons: Late Pleistocene to recent: *Earth and Planetary Science Letters*, v. 466, p. 70–79, <https://doi.org/10.1016/j.epsl.2017.03.001>.
- McDaniel, D.K., McLennan, S.M., and Hanson, G.N., 1997, Provenance of the Amazon Fan muds: Constraints from Nd and Pb isotopes, *in* Flood, R.D., et al., *Proceedings of the Ocean Drilling Program, Scientific results, Volume 155: College Station, Texas, Ocean Drilling Program*, p. 169–176.
- Mertes, L.A.K., and Dunne, T., 2007, Effects of tectonism, climate change, and sea-level change on the form and behaviour of the modern Amazon River and its floodplain, *in* Gupta, A., ed., *Large Rivers: Geomorphology and Management*: New York, John Wiley and Sons, p. 115–144, <https://doi.org/10.1002/9780470723722.ch8>.
- Milliman, J.D., and Farnsworth, K.L., 2011, *River Discharge to the Coastal Ocean: A Global Synthesis*: Cambridge, UK, Cambridge University Press, 384 p., <https://doi.org/10.1017/CBO9780511781247>.
- Moecher, D.P., and Samson, S.D., 2006, Differential zircon fertility of source terranes and natural bias in the detrital zircon record: Implications for sedimentary provenance analysis: *Earth and Planetary Science Letters*, v. 247, p. 252–266, <https://doi.org/10.1016/j.epsl.2006.04.035>.
- Normark, W.R., and Reid, J.A., 2003, Extensive deposits on the Pacific plate from Late Pleistocene North American glacial lake outbursts: *The Journal of Geology*, v. 111, p. 617–637, <https://doi.org/10.1086/378334>.
- Novello, V.F., et al., 2017, A high-resolution history of the South American Monsoon from Last Glacial Maximum to the Holocene: *Scientific Reports*, v. 7, 44267, <https://doi.org/10.1038/srep44267>.
- Pepper, M., Gehrels, G., Pullen, A., Ibañez-Mejía, M., Ward, K.M., and Kapp, P., 2016, Magmatic history and crustal genesis of western South America: Constraints from U-Pb ages and Hf isotopes of detrital zircons in modern rivers: *Geosphere*, v. 12, p. 1532–1555, <https://doi.org/10.1130/GES01315.1>.
- Saucier, R.T., 1996, A contemporary appraisal of some key Fiskian concepts with emphasis on Holocene meander belt formation and morphology: *Engineering Geology*, v. 45, p. 67–86, [https://doi.org/10.1016/S0013-7952\(96\)00008-7](https://doi.org/10.1016/S0013-7952(96)00008-7).
- Saylor, J.E., and Sundell, K.E., 2016, Quantifying comparison of large detrital geochronology data sets: *Geosphere*, v. 12, p. 203–220, <https://doi.org/10.1130/GES01237.1>.
- Sharman, G.R., and Johnstone, S.A., 2017, Sediment unmixing using detrital geochronology: *Earth and Planetary Science Letters*, v. 477, p. 183–194, <https://doi.org/10.1016/j.epsl.2017.07.044>.
- Spencer, C.J., Kirkland, C.L., Roberts, N.M.W., 2018, Implications of erosion and bedrock composition on zircon fertility: Examples from South America and Western Australia: *Terra Nova*, v. 30, p. 1–7, <https://doi.org/10.1111/ter.12338>.
- Sweet, M.L., and Blum, M.D., 2016, Connections between fluvial to shallow marine environments and submarine canyons: Implications for sediment transfer to deep water: *Journal of Sedimentary Research*, v. 86, p. 1147–1162, <https://doi.org/10.2110/jsr.2016.64>.
- Thomson, K.D., Stockli, D.F., Clark, J.D., Puigdefàbregas, C., and Fildani, A., 2017, Detrital zircon (U-Th)/(He-Pb) double-dating constraints on provenance and foreland basin evolution of the Ainsa Basin, south-central Pyrenees, Spain: *Tectonics*, v. 36, p. 1352–1375, <https://doi.org/10.1002/2017TC004504>.
- Vail, P.R., Mitchum, R.M., Jr., Todd, R.G., Widmier, J.M., Thompson, S., III, Sangree, J.B., Bubb, J.N., and Hatlelid, W.G., 1977, *Seismic stratigraphy and global changes of sea level*, *in* Payton, C.E., ed., *Seismic Stratigraphy—Applications to Hydrocarbon Exploration: American Association of Petroleum Geologists Memoir 26*, p. 49–212.
- Vermeesch, P., 2013, Multi-sample comparison of detrital age distributions: *Chemical Geology*, v. 341, p. 140–146, <https://doi.org/10.1016/j.chemgeo.2013.01.010>.

Printed in USA